Cover Page

Universiteit Leiden

The handle http://hdl.handle.net/1887/19743 holds various files of this Leiden University dissertation.

Author: Paul, Petra
Title: The systems biology of MHC class II antigen presentation
Date: 2012-09-06

Chapter 2

A Genome-wide Multi-Dimensional RNAi Screen Reveals Pathways Controlling MHC Class II Antigen Presentation

Supplemental Information

Cell. 2011 Apr 15;145(2):268-83

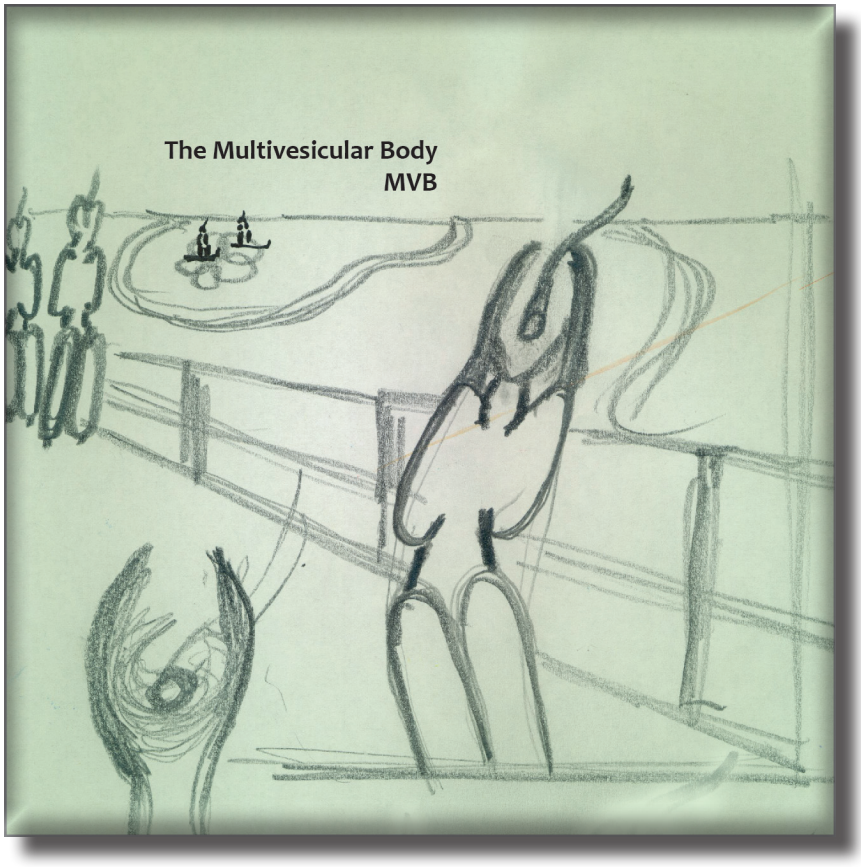

Supplemental Experimental Procedures

Cell Lines

Wild-type (wt) MelJuSo, human melanoma cell line, expressing HLA-DRB3 [17], was cultured in IMDM (Gibco) supplemented with 7.5% fetal calf serum (FCS, Greiner). MelJuSo were transfected with HLA-DRB1-GFP and mCherry-GalT2, stable clones were selected and cultured in IMDM/7.5% FCS supplemented with Penicillin/Streptomycin (Invitrogen), Hygromycin (Invitrogen) and Neomycin/G418 (Gibco). Human 293T cells were cultured in DMEM (Gibco) supplemented with 7.5% fetal calf serum (FCS, Greiner) and Penicillin/Streptomycin (Invitrogen).

Constructs

HLA-DRB1-GFP from pCDNA3-DR1B-GFP [18] was cloned into pCDNA3 via HindIII-XhoI. GalT2 was removed via EcoR1-BamH1 from GalNac-T2-GFP [19] construct (generous gift from T. Nilson) and placed into pmCherry-C1, where we replaced GFP from pEGFP-C1 [20] (Clontech) for mCherry via NheI and BglI.

The packaging constructs used for lentivirus production are as follows, pMDLg/pRRE, pRSV-Rev and pCMV-VSV-G [21], kindly provided by Dr. M. Soengas (University of Michigan, USA). The pLKO.1 plasmids containing shRNA hairpins targeting selected genes were purified from bacterial glycerol stocks (Open Biosystems, Thermo Scientific) using a large scale plasmid DNA purification kit (Qiagen). The vectors pLKO.1 empty, pLKO.1 EGFP shRNA, pLKO.1 TurboGFP shRNA, pLKO.1 Luciferase shRNA and pLKO.1 non-target shRNA served as negative controls.

ARL14/ARF7 Q68L missing the sequence coding for the myristoylation site (first two N-terminal amino acids) was amplified from IMAGE: 4747382 and cloned into pGBT9 via EcoRI and BamH1 restriction sites to use for Yeast Two-Hybrid assay. ARL14/ARF7 was cloned, using restriction sites EcoRI and BamHI, into pRP265 and mCherry-N1 via EcoRI and BamHI. ARF7EP was amplified form IMAGE clone 6062049 and cloned into pRP265 and p2HA-C1 via BglII and EcoRI (p2HA-C1 was retrieved from pEGFP-C1 (Clontech) where GFP was exchanged for HA-HA using Nhe1 and BglII cloning sites). Those constructs were used for protein production, co-immune precipitation and colocalization experiments. SEC7 domains of PSD4 (aa555-aa738) and CYTH1 (aa73-aa202) were amplified from IMAGE clone 5757431 (PSD4) and IMAGE clone 4755203 (CYTH1) and cloned into pMAL-c2X using BamHI and HinDIII restriction sites. Double PH-domains of PSD4 (aa776-aa892) were amplified and cloned into pRP265 and pEGFP-N1 using BglII, EcoRI and BamH1 for lipid binding. pGEX-Arf6 was a generous gift from Dr. C. D'Souza-Schorey (University of Notre Dame, FR). GFP-PIP5K1A GFP was a generous gift from Dr. N. Divecha (The University of Manchester,UK) [22]. Myo1E and Myo1E tail (aa710-aa1109) both amplified from IMAGE clone 30527536 were cloned into pEGFP-C1 using Asp718I and BamHI as restriction sites.

Antibodies

The hybridoma cell lines L243 (anti-HLA-DR complex, ATCC) and CerCLIP.1 (anti-CLIP24) have been described previously [23, 24]. Cells were maintained in IMDM/7.5% FCS, penicillin/streptomycin and gentamycin (Gibco). The monoclonal antibodies were purified, concentrated by HPLC and affinity purified using protein G-sepharose beads (Amersham Biosciences). L243 and CerCLIP antibodies were directly conjugated to Cy3 and Cy5 fluorophores, respectively and purified by size exclusion chromatography.

Mouse anti-human EEA1 (MAB 610457, BD transduction laboratories), Hoechst (2 µg/ml, 33342, Invitrogen), Phalloidin-Alexa568 (0.4 U/ml, Molecular Probes), mouse anti-human CD63 NKI-C3 [25], mouse anti-human Arl14 (BioConnect), mouse anti B-actin (AC-15, Sigma Aldrich) and rabbit anti-human HLA-DR [26, 27] were used to stain early endosomes, nuclei, actin, CD63, FLJ22595 (Arl14/ARF7), B-actin and HLA-DR, respectively, followed by secondary Alexa dye-coupled antibodies (Invitrogen) for detection by confocal microscopy.

Antibodies against human Arl14/Arf7 (ARL14.2) and human ARF7EP (used for immune precipitation, western blotting and immune fluorescence) were produced in rabbits after immunization with recombinant GST-Arl14/Arf7 and GST-ARF7EP respectively (GST was removed by Thrombin cleavage). Anti-HA (12CA5, gift from Dr. H. Ovaa, NKI, Amsterdam, NL) was used for co-immune precipitation assays. Rabbit anti-human Myo1E (H-60, Santa Cruz Biotechnology), mouse anti-GST (B14, Santa Cruz, sc-138), rabbit anti-mRFP, rabbit anti-GFP [28] and anti-HA-PO (Roche, 2013819001) were used for detection on Western Blot. Rabbit anti-mRFP was also used for immune precipitation.

Flow Cytometry HTS: RNAi Screen Layout

In the primary screen siRNAs (Human siGenome siRNA SMARTpool library - Genome, Dharmacon) were used to silence human genes in MelJuSo cells. In the deconvolution screen, the four siRNA duplexes of the smartpool of a potential candidate were tested separately. All steps were performed in triplicate. MelJuSo untreated and HLA-DM siRNA transfected were used as negative and positive

control (for CerCLIP), respectively.

Flow Cytometry HTS: siRNA Transfection

siRNA (50 nM final concentration) was aliquoted into 96-well plates (Greiner CELLSTAR® 96-well microplates, black, flat bottom) using a liquid handling robot (Hamilton ML STAR). Per well, 0.2 µl DharmaFECT1 (Dharmacon) and 9.8 µl IMDM was added to the siRNA, incubated for 20 minutes, followed by addition of 4,700 MelJuSo cells using a Microplate Dispenser (Matrix WellMate®) and culture for three days at 37°C and 5% CO2 before analysis.

Flow Cytometry HTS: Analysis

Cells were washed with PBS (Gibco), detached using 10 µl/well Trypsin-EDTA (Gibco) and incubated with 5 µg/ml L243-Cy3 and 6.7 µg/ml CerCLIP-Cy5 in 20 µl/well PBS/2% FCS for 30 minutes at 4°C. Samples were diluted to 200 µl with PBS/2% FCS, followed by 10 minutes incubation on ice before the mean fluorescence intensity (MFI) was determined using the BD FACSArray™ Bioanalyzer System (Becton Dickinson).

Flow Cytometry HTS: Normalization

Raw flow cytometry data (geometric mean fluorescence intensity of each antibody) was normalized using the CellHTS2 package of R2.6.0-based Bioconductor [29]. All data points were transformed into z-scores. The average z-score and standard deviation of untreated MelJuSo cells were calculated. Genes displaying a |z-score|>3 in at least two replicates were regarded as 'candidates'. In the deconvolution screen a candidate was considered confirmed, when at least two duplexes reproduced the phenotype observed in the primary screen.

Microarray Analysis

Human primary monocytes as well as immature and mature monocyte-derived DC were isolated and differentiated as described [30]. Human primary B cells were isolated from peripheral blood and activated as described [31]. Detailed protocols for RNA isolation, amplification, labeling, and hybridization can be found at **http://cmf.nki.nl/download/protocols.html**. The Sentrix Human-6_v.2 BeadChip (Illumina) was used for the whole genome gene expression study. The data underwent variance stabilizing transformation and robust spline normalization. Candidates were considered expressed in immune cells with a detection p-value of 0.01 or lower. Expression of a gene in at least one of five primary cell types led to incorporation in the deconvolution screen.

Data on overall gene expression in 79 human tissues was obtained from Novartis GNF SymAtlas (**http://biogps.gnf.org**). The GC-RMA package processed data was LOG-transformed. Expression maxima for immune versus normal tissues were determined and ranking upon the ratio was performed. Immune-specific expression threshold was set above a ratio of 1.09, which corresponded to that of CIITA.

Quantitative RT-PCR

Messenger RNA was extracted from cells using the mRNA Capture Kit (Roche) and reverse transcribed into cDNA using the Transcriptor High Fidelity cDNA Synthesis Kit (Roche). The qPCR was performed using LightCycler® 480 SYBR Green 1 Master (Roche) on the LightCycler® 480 Detection System (Roche). Primer sequences are available upon request. Quantification was performed using the comparative CT method (ΔΔCT). The results were expressed relative to GAPDH values; normalized to control siRNA treated cells and LOG-transformed. In case of lentiviral-transduced DC, results were expressed relative to 18S rRNA values and normalized to shControl treated cells

Confocal Microscopy HTS: siRNA Transfection

MelJuSo/HLA-DRB1-GFP/mCherry-GalT2 cells were transfected with siRNAs silencing all 276 candidates as described above and seeded on µ-Slide 18-well plates (flat ibiTreat, Ibidi). Control siRNA and RILP#3 siRNA, which separates the late endosomal Rab7-RILP receptor from the dynein motor resulting in scattered MHC class II-positive vesicles [32], were used as negative and positive control, respectively.

Confocal Microscopy HTS: Analysis

Cells were fixed with PBS/3.75% formaldehyde (free from acid, Merck), permeabilized with PBS/0.1% TritonX-100 (Sigma) and blocked with PBS/0.5% bovine serum albumin (BSA, Sigma). Cells were stained with anti-EEA1, goat anti-mouse-Alexa647 and Hoechst, washed with PBS and covered with 80% glycerol (Merck) in PBS. Stained cells were analyzed by a Leica AOBS microscope with appropriate filters for fluorescence detection. Pictures were taken using a HCX PL APO blue corrected 63x 1.32 object. Hoechst was excited at l=405nm and detected at l=416-470nm; GFP was excited at l=488nm and detected at l=500-550nm; mCherry was excited at l=561nm and detected at l=570-621 nm; Alexa-647 was excited at l=633nm and detected at l=642-742nm.

Confocal Microscopy HTS: CellProfiler and Clustering

Cell image analysis program CellProfiler 1.0.5811, as provided by the Broad Institute (Boston, USA), was used to extract multiple features from the cells in each image [33]. Briefly, nuclei were detected as primary objects. From these nuclei the cell was detected based on cytosolic background staining. EEA1 and MHC class II vesicles and the Golgi were detected as primary objects and then assigned to a cell containing this object (their parent). The membrane area was defined as the area between the cell perimeter expanded or shrunken by 10 pixels. The CP Analyst 2 program was used to determine the minimal number of parameters distinguishing and describing phenotypes of interest. During supervised machine learning seven bins for MHC class II, three for early endosome and five for Golgi features were designed. After cross-validation accuracy calculation (Figure S4B) six MHC class II parameters, two for EEA1 and five for Golgi were selected. All these features were z-score normalized in Excel (Table S4). The MHC class II related parameters were replicated four times and the Golgi related parameters were replicated two times to increase their weight in the consideration. A similarity matrix was calculated and the data were clustered using the Matlab Bioinformatics Toolbox. The phylogenetic tree was build in Matlab and imported into Cytoscape (2.6.3) with the PhyloTree (v.0.1) plug-in. The tree was plotted as an organic tree and nodes were coloured according to the z-score in the flow cytometry-based screen. The edge colour was determined by the changes in mRNA levels between im and mDCs (Table S1). The node size was determined by the mDC like phenotype, which is based on microscopy data (Table S4). Two bins were created in CP Analyst 2: one with wild type cells and one with cells resembling an mDC phenotype (MHC class II at the cell surface and little MHC class II inside). All cells for each candidate were scored for the enrichment of the mDC phenotype.

Confocal Microscopy HTS: Network Analysis

Humannet v. 1 [16] was used to predict genes that interact with candidate genes (neighbours). Two cut-off values were applied to be considered as an interacting gene: neighbours have a log-likelihood score ≥1 and a $|z| \geq 1.645$ in the flow cytometry screen. All candidates or clusters (with or without neighbours) were analyzed for enrichment in Gene Ontology terms (Cellular Component). Clusters were defined by having a distance of 153.6 from the root of the tree and at least 15 genes in the branch. Gene Ontology analysis was performed with the cytoscape plug-in BiNGO (v.2.3).

Lentivirus Production

Lentiviruses were produced as described previously [34] with following alterations. 293T cells were seeded at 3.5x106 per 10 cm dish 24 h before transfection in DMEM/7.5% FCS/PS. 293T cells were transiently transfected with the viral packaging constructs pMDLg/pRRE, pRSV-Rev and pCMV-VSV-G (ratio 1:1:1) in a ratio of 1:1 with the pLKO.1 vector harboring the respective shRNA sequence using 4 µl Fugene 6 transfection reagent (Roche) per µg of DNA. Per 10 cm dish, 2.33 µg of each packaging vector, 6.5 µg of pLKO.1 and 0.5 µg of pEGFP-C1 [20] (Clontech) were used. After 24 h the complete medium was replaced by serum-free DMEM. After another 24 h of culture, the supernatant was harvested and concentrated 100-fold by ultracentrifugation (Beckman Coultor Rotor SW28) at 20,000 rpm for 2 h at room temperature. The viral pellet was resuspended in Cellgro medium (Cellgenix), snap frozen in liquid nitrogen and stored at -80°C.

Dendritic Cell Transduction

Human primary monocytes were isolated from peripheral blood of healthy volunteers after informed consent as described [30], frozen and stored in liquid nitrogen. Thawed monocytes were plated at one million per well in 12 well plates (Falcon) and transduced with lentivirus at a MOI of 2 in 1 ml Cellgro medium in the presence of 4 µg/ml polybrene (Millipore). The medium was supplemented with 800 U/ml IL-4 and 1,000 U/ml GM-CSF (Cellgenix). After 24 h, 1 ml of Cellgro plus IL-4 and GM-CSF was added again. Cells were cultured for six days at 37°C and 5% CO_2 before analysis by flow cytometry. Maturation of DC was induced at day 5 by adding 10 ng/ml IL-1β, 10 ng/ml TNF-α, 1,000 U/ml IL-6 (Cellgenix) and 1 µg/ml PGE_2 (Sigma). For immunofluorescence, DC were seeded on µ-Slide 18-well plates (Ibidi) pre-coated with 20 µg/ml Fibronectin (Invitrogen) and incubated for seven hours. Slides were fixed with PBS/3.75% formaldehyde and stained with anti-HLA-DR and anti-CD63 antibodies, phalloidin and Hoechst. The "Measure Correlation" module of CellProfiler was used to determine the correlation between CD63 and MHC class II localisation. Correlation pixel plots were determined using the Leica Confocal Software.

Biochemical Experiments: Yeast Two-Hybrid Analysis

Arl14/ARf7 Q68L without myristoylation site was used as bait in a Yeast Two-Hybrid assay that was performed in a skeletal muscle cDNA library at DKFZ,

Heidelberg, Germany (information: **http://www.dkfz.de/gpcf/y2h.html**). Results are listed in Table S7.

Biochemical Experiments: Immune Precipitation and Pull-down

Cells (PBMC or MelJuSo) were lysed for 30 min in 0.8% NP-40 lysis buffer containing 50 mM NaCl, 50 mM Tris-HCl pH8.0, 5 mM $MgCl_2$ and phosphatase inhibitors (Roche Diagnostics, EDTA free). Supernatant after spinning (10 min at max. speed) was incubated with GST- or GST-ARF7EP-coupled Glutathione Sepharose beads 4G (GE Healthcare) or with anti-ARF7EP-, anti-mRFP- and anti-HA-coated Protein G-Sepharose beads 4 Fast flow (GE Healthcare) for one hour. Beads were washed four times before addition of Laemmli Sample Buffer followed by 5 min incubation at 100°C. Detection of co-immune-precipitated proteins was done via SDS-PAGE followed by western blotting and probing with respective antibodies to visualize proteins.

Biochemical Experiments: Immune Fluorescence

imDC were seeded on µ-Slide 18-well plates (Ibidi) pre-coated with 20 µg/ml Fibronectin (Invitrogen) and incubated for seven hours, fixed with 3.7% Formaldehyde in PBS or methanol and stained for MHC class II, Arl14/Arf7 and B-Actin. MelJuSo cells were transfected using FuGENE 6 (Roche Diagnostics) with DNA coding for Arl14/Arf7-mCherry and GFP-PIP5K1A followed by fixation with 3.7% formaldehyde in PBS two days post-transfection and staining for MHC class II.

Biochemical Experiments: GEF Assay

Ten µM GST-ARF6, GST-ARL14 or GST in loading buffer (1 mM EDTA, 4 mM $MgCl_2$, 50 mM HEPES pH7.6, 1 mM DTT) were incubated with 100 µM MBP-SEC7 domain of CYTH1 or PSD4 in loading buffer. Then, 3.3 µM) [α-32P]GTP (>5000 Ci/mmol) was added and incubated at 30°C for 20 min. The reactions were stopped by adding 500 µl cold stop buffer (100 mM NaCl, 10 mM $MgCl_2$, 20 mM HEPES pH7.6) and 20 µl Glutathione beads. The beads were washed five times with stop buffer to remove unbound [α-32P] GTP and measured by liquid scintillation counting. Free GST was taken as background and subtracted from all measurement values.

Biochemical Experiments: Lipid Binding Assay

HEK293T cells transiently overexpressing GST-PH-PH (PSD4) were harvested in 0.1% NP-40 lysis buffer, containing 50 mM Tris-Cl (pH7.4), 100 mM NaCl, 5 mM $MgCl_2$ and protease inhibitors. Cells were frozen at -80°C and thawed again followed by sonication. Lysis was extended for 45 min at 4°C. The supernatant after centrifugation was added to Glutathione Sepharose beads 4B to isolate GST-PH-PH (PSD4) from the lysate. Beads were washed two times, GST-PH-PH (PSD4) was eluted from beads using 100 mM Glutathione and used for the Lipid Binding assay.

PIP-StripsTM (tebu-bio) were blocked in PBS containing 3% fatty acid free BSA (Sigma # A-7030). The PIP-Strip was incubated with GST-PH-PH (PSD4) and the positive control (PLC-δ1 PH domain, PI(4,5)P_2 GRIPTM, tebu-bio) overnight. Binding to phosphoinositides was visualized by incubation with anti-GST antibody (B-14, Sc138 from Santa Cruz).

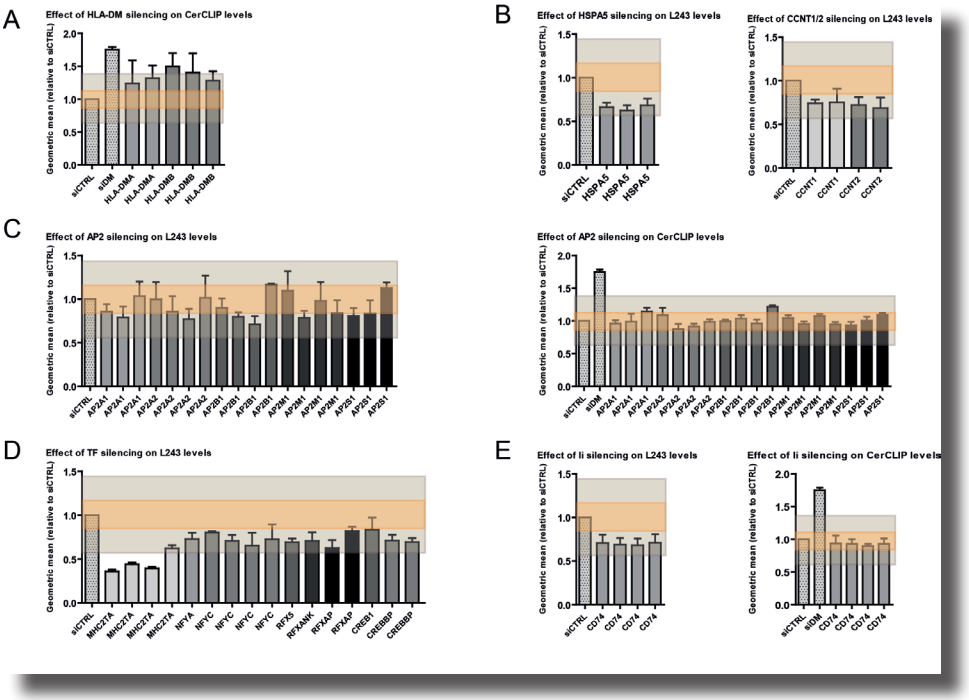

Figure S1 | Deconvolution of Genes known to affect the MHC Class II Pathway. Relates to Figure 2 (Chapter 1)
This figure explains the absence of genes known to be involved in the MHC class II pathway from our candidate list. Orange box: |z-score|<1; gray box: |z|<3. Representative, non-toxic siRNA duplexes are shown.
A | HLA-DM consists of an α and β chain and acts as a chaperone for MHC class II loading. While HLA-DMB showed a significant effect, HLA-DMA did not. For HLA-DMB, three siRNA duplexes show upregulation of CerCLIP labelling, two of which by a |z|>3 (our threshold). When silencing HLA-DMA only two duplexes gave an effect just below our threshold.
B | Some siRNA duplexes against HSPA5 (BiP, a chaperone in the ER that binds newly synthesized MHC class II) or CCNT1/CCNT2 (Cyclin T1/T2, both components of the transcriptional elongation complex PTEFb, which binds CIITA to turn on MHC class II transcription) showed a decrease in L243, but their effect was below the threshold.
C | Subunits of AP2 (Adaptor Protein 2 complex which is involved in the trafficking of MHC class II molecules) were not identified in the screen because silencing of individual subunits does not influence L243 or CerCLIP levels.
D | CIITA showed a pronounced effect, but the other factors involved in MHC class II transcription like NFY, RFX and CREB did not. As the deconvolution shows, silencing of these genes decreases L243 levels, but only with a z-score below our threshold of |z|>3.
E | Invariant chain (CD74) silencing also decreased L243 levels, but again below the threshold. No effect on CerCLIP levels was found.

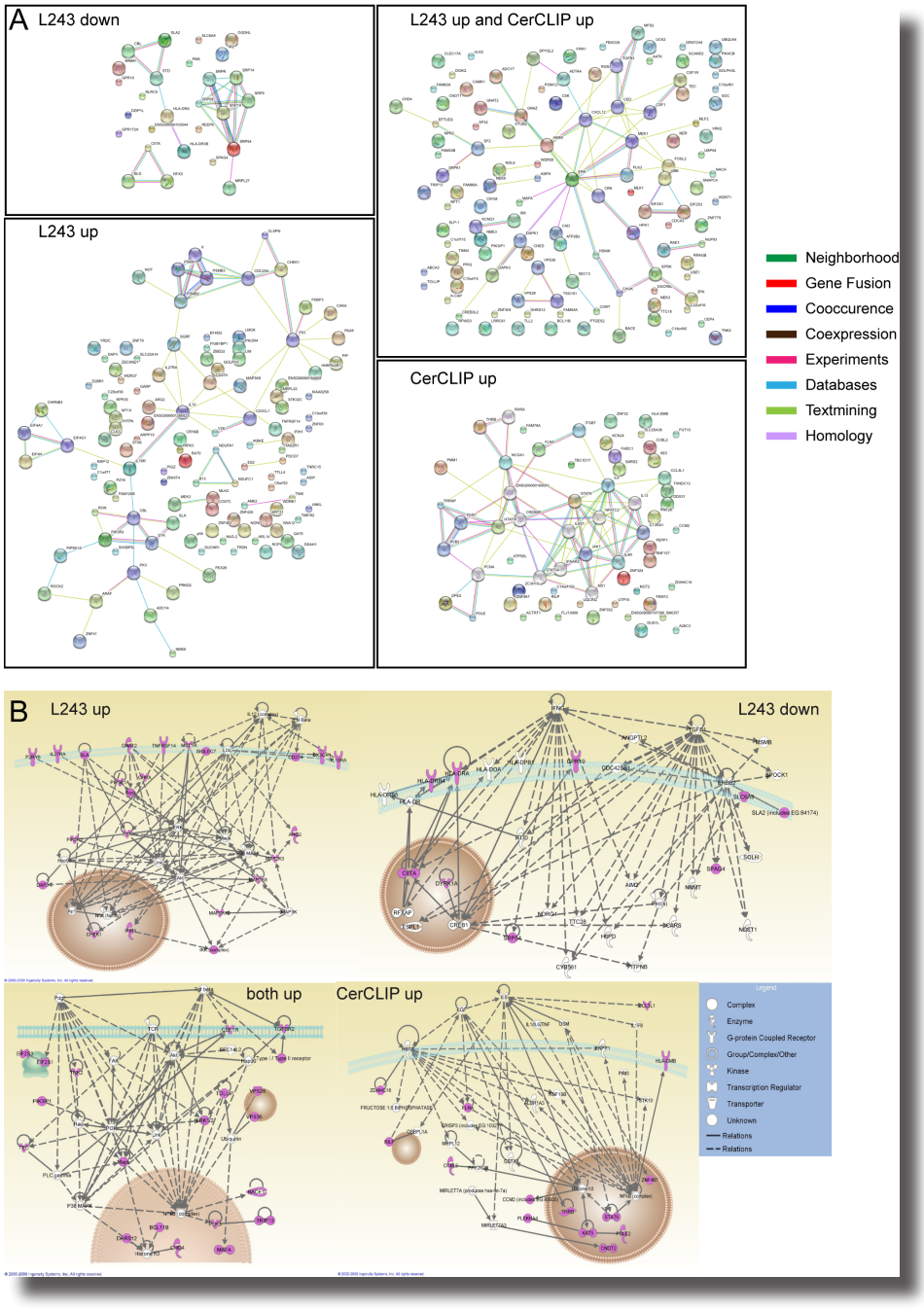

Figure S2 | Pathway Analysis of Targets grouped according to the Effects observed in the Primary Screen. Relates to Figure 2 (Chapter 1)

The 276 targets were grouped according to their effect on MHC class II at the cell surface. These four clusters (L243 up, L243 down, CerCLIP up and L243/CerCLIP up) were analyzed using the open source database and network program String (A) and the Ingenuity Pathways Analysis (IPA) program (B), resulting in networks summarized in this figure. Candidates identified in the screen are highlighted in pink in IPA-derived networks.

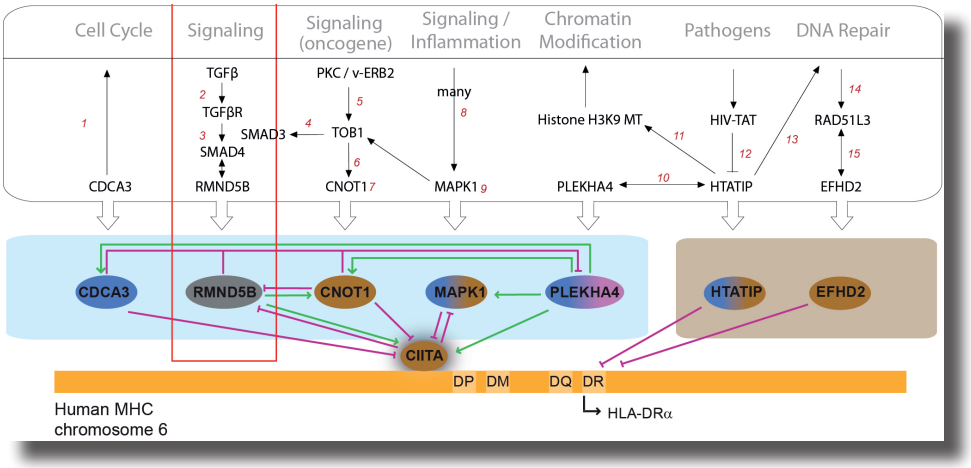

Figure S3 | Higher Order Control of the transcriptional Network. Relates to Figure 3 (Chapter 1)
Based on literature and experimental data (red box), factors interacting with candidates involved in transcriptional control and pathways were annotated in more general terms. Numbers correspond to Supplemental References [1-15].

A

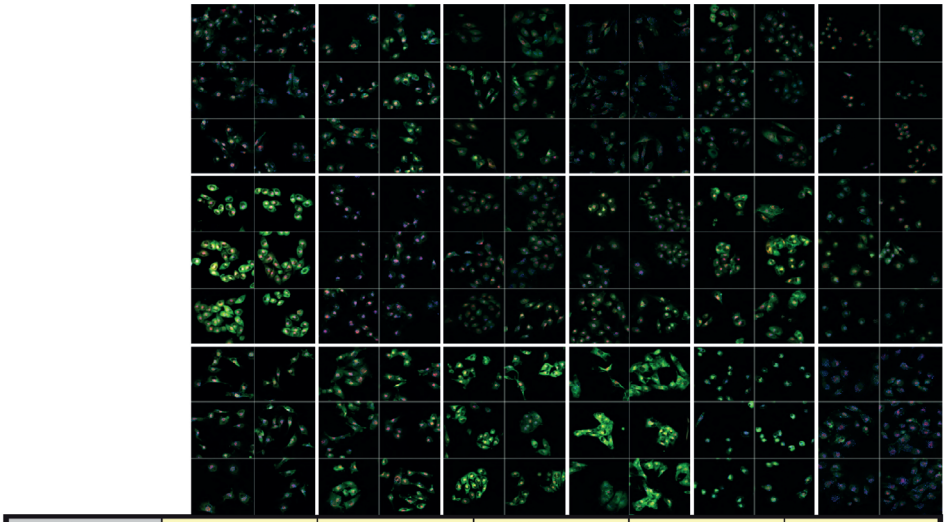

neg. control	HLA-DMB	THTPA	LOC403313	CHKA	DAPK3
pos. control	ASP	CAMK1	CDC2L5	PLK3	CSF1R
MAP3K11	MAP3K12	MAP3K14	MAP3K9	MAP4K1	MAPK1

B

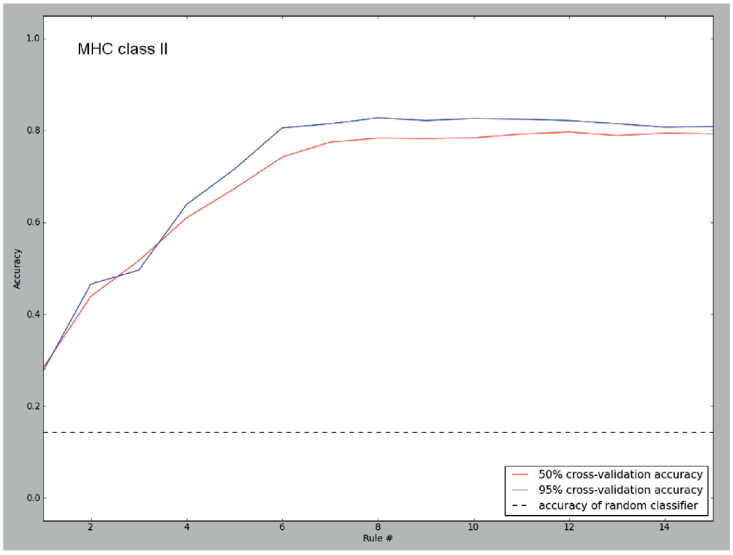

Figure S4 | Confocal Microscopy Image Analysis and 'Supervised Machine Learning'. Relates to Figure 4

A | MelJuSo/HLA-DRB1-GFP (green)/mCherry-GalT2 (red) cells were transfected with siRNAs silencing all 276 candidates and seeded on µ-Slide 18-well plates. After three days cells were stained for early endosomes (blue). On representative slide is shown. High resolution images of all slides can be found on ***http://www.neefjeslab.nl/****.*

B | Confocal images after gene silencing were analyzed by Cell Profiler. Prominent phenotypes were identified and the Cross-Validation Accuracy for MHC class II parameters after supervised machine learning in CP Analyst 2 was determined. Accuracy to distinguish defined phenotypes does not increase when more than six parameters are used.

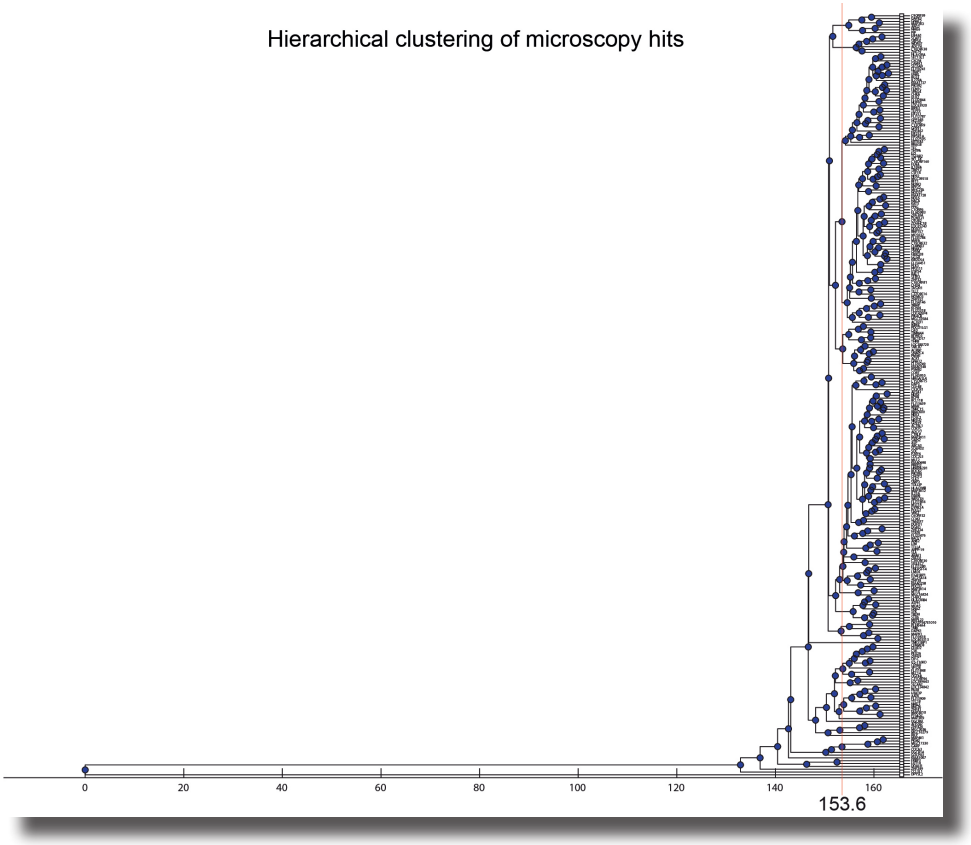

Figure S5 | Hierarchical Clustering of Microscopy Data. Relates to Figure 4C and 5 (Chapter 1)
The (dis)similarity between phenotypes upon knockdown of different genes is represented in this hierarchical clustering. A distance of 153.6 to the root of the tree was arbitrarily chosen as a cut-off value. Branches with more than 14 genes were used for further analysis (Figure 4C, Chapter 1).

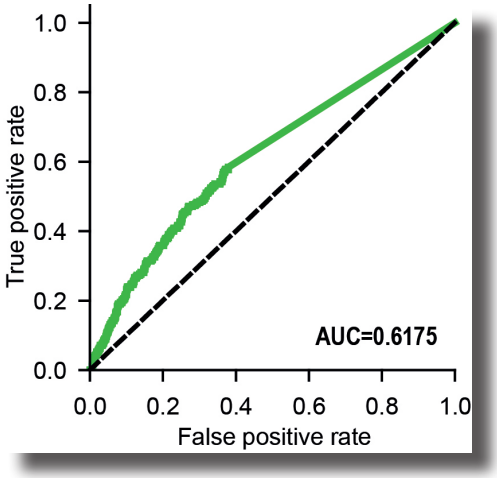

Figure S6 | The connectivity targets measured by the Area Under the Receiver Operating Characteristic (ROC) Curve (AUC) determined by program humannet v.1. Relates to Figure 5 (Chapter 1)
With an AUC of 0.6175 many of the connected genes (neighbours) are highly expected to interact in reality. Neighbours with a log-likelihood score ≥1 and a |z| ≥1.645 (p<0.1) in our original flow cytometry-based screen were considered for further analysis (Table S6).

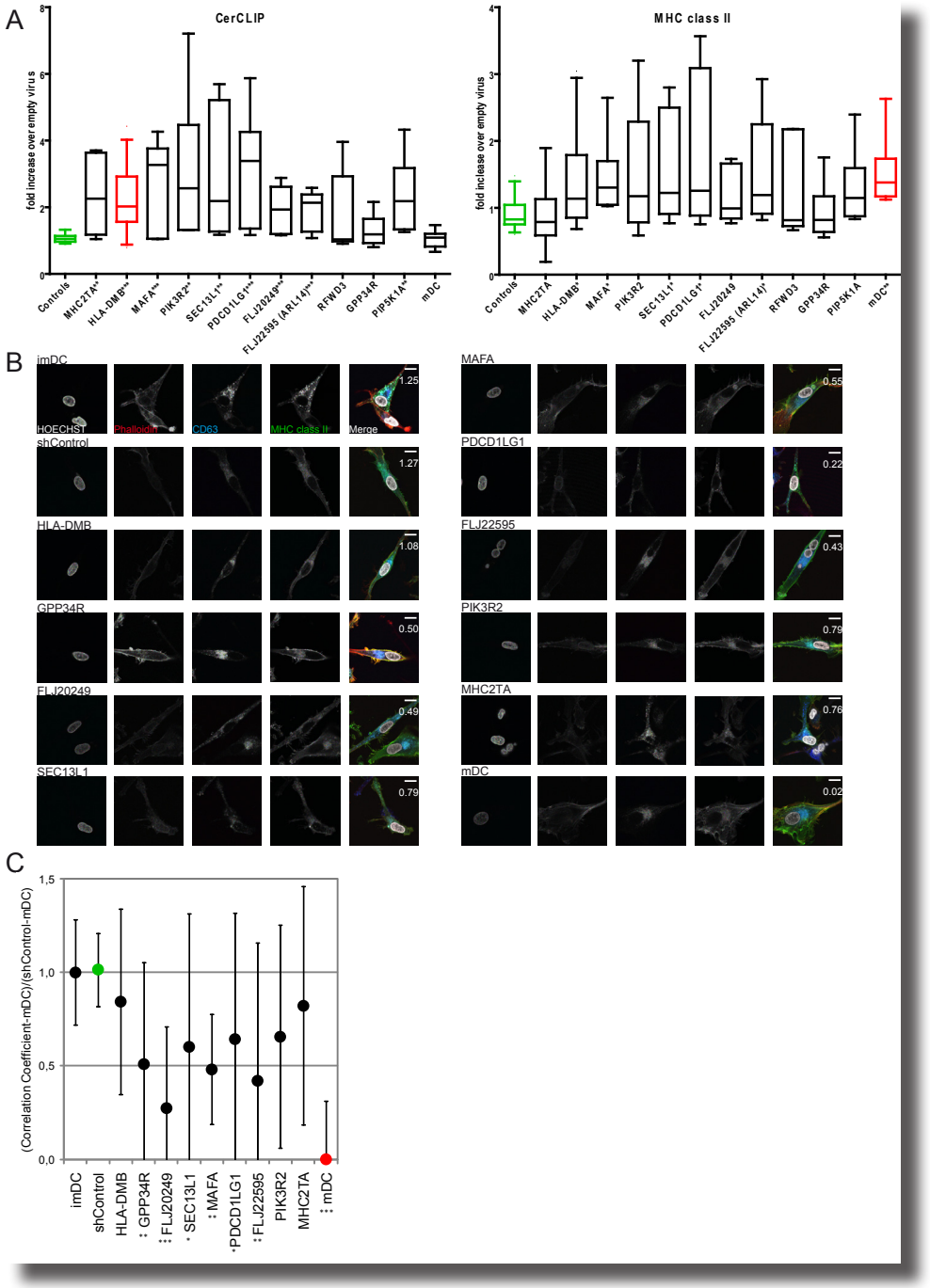

Figure S7 | Effect of selected Candidates on the Redistribution of MHC Class II in Dendritic Cells. Relates to Figure 6 (Chapter 1)

Monocytes were transduced with lentiviruses encoding shRNAs directed against seven candidate genes (four shRNA constructs per gene). After six days, imDCs generated from the transduced monocytes were analysed.

Supplemental Tables 1-7

available online at **http://dx.doi.org/doi:10.1016/j.cell.2011.03.023**

Table S1 | Expression of Candidates in human primary Immune Cells and Tissues, Relates to Figure 1 and 2 (Chapter 1)
mRNA of five different human primary immune cells (unstimulated and CD40L-activated B cells, primary monocytes, immature and mature monocyte-derived DC) was isolated and submitted to microarray analysis to investigate the expression levels of the candidates from the primary siRNA screen. The cells were characterized by flow cytometry for their lineage, MHC class II expression and activation status (data not shown). This table represents the average signal and the detection p-value of the microarray analysis. Probes for some of the hits were absent from the array as indicated at the bottom of the table. Gene expression data for 79 human tissues was retrieved from the GNF SymAtlas database. The detection signals are represented in this table divided into immune and non-immune tissues. The maxima for each group are determined and a ratio of 1.09 (as for CIITA) or higher is considered 'immune tissue-specific'. Sixty-nine hits fall into this group (highlighted in green).

Table S2 | Summary of the Results after Deconvolution, Relates to Figure 1 and 2 (Chapter 1)
The primary screen was performed using a pool of four siRNA duplexes per gene from a Dharmacon library. For deconvolution, the candidates were silenced using the four individual duplexes. This table summarizes the measured effects of each annotated siRNA pool and the number of duplexes confirming the phenotype in the pool of four siRNAs (for both L243 and CerCLIP, separately). The function and the cellular localization of the candidates were extracted from the Ingenuity Pathways Analysis program.

Table S3 | Description of Factors acting in a Transcriptional Network on the MHC Class II Locus identified by HTS qPCR, Relates to Figure 3 (Chapter 1)
Information based on published literature.

Table S4 | Summary of HTS Microscopy Results after Cell Profiler Calculation and CP Analyst 2 classification including mDC Phenotype Enrichment Score, Relates to Figure 4 (Chapter 1)
Six confocal microscopy pictures for each siRNA silencing situation were analyzed using Cell Profiler. After manual selection for prominent phenotypes and 'supervised machine learning', the most descriptive parameters for these phenotypes were determined. Per annotated gene, the values for the selected parameters used for clustering are listed in this table. Two bins were created in CPanalyst. One with wild type cells and one with cells resembling an mDC phenotype (MHC class II at the cell surface and little MHC class II inside). All cells for each candidate were scored for the presence of these two phenotypes. The p value for the mDC phenotype is indicated.

Table S5 | Gene Ontology Analysis of all our Candidate Genes. Relates to Figure 5 (Chapter 1)
The p value for 'cellular component' terms that are enriched in our dataset are given. The p values for 'cellular component' terms that are enriched in our dataset (extended with their neighbours) are given.

Table S6 | Genes connected to the Candidate Genes (Neighbours). Relates to Figure 5 (Chapter 1)
Humannet v. 1 was used to predict genes (Entrez Gene ID) that are likely to interact with candidate genes [16]. For each of the four clusters potentially interacting genes are indicated with the number 1. Each potentially interacting gene has at least a minimal absolute z-score of 1.645 (p=0.1) in the

Figure S7 | continued
A | Fold increase in CLIP-loaded MHC class II (CerCLIP) or general MHC II levels as detected by flow cytometry of three donors normalized to cells transduced with empty viral particles is shown. Four non-targeting shRNA sequences were used as shControl. HLA-DMB represents a positive control for the increase of CerCLIP, whereas L243 levels on mDCs can be considered as maximum. Shown is the 10-90 percentile with median value.
B | Representative images of all candidates silenced by lentiviral transduction of imDC, which confirmed their flow cytometry phenotype of MelJuSo cells in imDCs are shown. Confocal images stained for nucleus, actin (Phalloidin), CD63 and MHC class II were taken. The normalized correlation coefficient of CD63 and MHC class II is stated in the merged image (average of shControl treated DCs equals 1, average of mDCs equals 0). Bar = 10µm
C | The correlation between CD63 and MHC class II was quantified using Cell Profiler. Ten images were taken per construct per donor. Correlation coefficients were normalised to shControl treated cells. Mean of all donors ± s.e.m. is shown for one out of four constructs. The two controls (HLA-DMB and MHC2TA) show no significant effect, whereas all tested candidates (except PIK3R2) show a significant correlation towards a mature DC phenotype in their MHC class II distribution.
*A, C | * p<0.05, ** p<0.01, *** p<0.0001, Student's t test.*

genome wide flow cytometry screen for effects on L243 and/or CerCLIP.

Table S7 | Proteins binding to Arl14 as detected in Yeast Two-Hybrid Assay. Relates to Figure 7 (Chapter 1)

All different preys picked up in Yeast Two-Hybrid assay with constitutive Arl14 used as bait. C11orf46, shaded in green and called ARF7EP in this study, was picked up 10 times. Three other interacting proteins (yellow) were found only once. The false positive preys (promiscuous preys and fragments from the 3' UTR) are depicted in orange.

References

1. Xaus, J., et al., *The expression of MHC class II genes in macrophages is cell cycle dependent.* J Immunol, 2000. **165**(11): p. 6364-71.
2. Piskurich, J.F., et al., *Identification of distinct regions of 5' flanking DNA that mediate constitutive, IFN-gamma, STAT1, and TGF-beta-regulated expression of the class II transactivator gene.* J Immunol, 1998. **160**(1): p. 233-40.
3. Massague, J. and D. Wotton, *Transcriptional control by the TGF-beta/Smad signaling system.* EMBO J, 2000. **19**(8): p. 1745-54.
4. Xiong, B., et al., *Tob1 controls dorsal development of zebrafish embryos by antagonizing maternal beta-catenin transcriptional activity.* Dev Cell, 2006. **11**(2): p. 225-38.
5. Suzuki, T., et al., *Phosphorylation of three regulatory serines of Tob by Erk1 and Erk2 is required for Ras-mediated cell proliferation and transformation.* Genes Dev, 2002. **16**(11): p. 1356-70.
6. Miyasaka, T., et al., *Interaction of antiproliferative protein Tob with the CCR4-NOT deadenylase complex.* Cancer Sci, 2008. **99**(4): p. 755-61.
7. Rountree, M.R., K.E. Bachman, and S.B. Baylin, *DNMT1 binds HDAC2 and a new co-repressor, DMAP1, to form a complex at replication foci.* Nat Genet, 2000. **25**(3): p. 269-77.
8. Kyriakis, J.M. and J. Avruch, *Mammalian mitogen-activated protein kinase signal transduction pathways activated by stress and inflammation.* Physiol Rev, 2001. **81**(2): p. 807-69.
9. Yao, Y., et al., *ERK and p38 MAPK signaling pathways negatively regulate CIITA gene expression in dendritic cells and macrophages.* J Immunol, 2006. **177**(1): p. 70-6.
10. Stelzl, U., et al., *A human protein-protein interaction network: a resource for annotating the proteome.* Cell, 2005. **122**(6): p. 957-68.
11. Sapountzi, V., I.R. Logan, and C.N. Robson, *Cellular functions of TIP60.* Int J Biochem Cell Biol, 2006. **38**(9): p. 1496-509.
12. Creaven, M., et al., *Control of the histone-acetyltransferase activity of Tip60 by the HIV-1 transactivator protein, Tat.* Biochemistry, 1999. **38**(27): p. 8826-30.
13. Hejna, J., et al., *Tip60 is required for DNA interstrand cross-link repair in the Fanconi anemia pathway.* J Biol Chem, 2008. **283**(15): p. 9844-51.
14. French, C.A., C.E. Tambini, and J. Thacker, *Identification of functional domains in the RAD51L2 (RAD51C) protein and its requirement for gene conversion.* J Biol Chem, 2003. **278**(46): p. 45445-50.

15. Martin, V., et al., *Sws1 is a conserved regulator of homologous recombination in eukaryotic cells.* EMBO J, 2006. **25**(11): p. 2564-74.
16. Kim, W.K., C. Krumpelman, and E.M. Marcotte, *Inferring mouse gene functions from genomic-scale data using a combined functional network/ classification strategy.* Genome Biol, 2008. **9 Suppl 1**: p. S5.
17. Johnson, J.P., et al., *Surface antigens of human melanoma cells defined by monoclonal antibodies. I. Biochemical characterization of two antigens found on cell lines and fresh tumors of diverse tissue origin.* Eur.J.Immunol., 1981. **11**(10): p. 825-831.
18. Wubbolts, R., et al., *Direct vesicular transport of MHC class II molecules from lysosomal structures to the cell surface.* J.Cell Biol., 1996. **135**(3): p. 611-622.
19. Storrie, B., et al., *Recycling of golgi-resident glycosyltransferases through the ER reveals a novel pathway and provides an explanation for nocodazole-induced Golgi scattering.* J Cell Biol, 1998. **143**(6): p. 1505-1521.
20. Shaner, N.C., et al., *Improved monomeric red, orange and yellow fluorescent proteins derived from Discosoma sp. red fluorescent protein.* Nat Biotechnol, 2004. **22**(12): p. 1567-1572.
21. Dull, T., et al., *A third-generation lentivirus vector with a conditional packaging system.* J Virol, 1998. **72**(11): p. 8463-8471.
22. Divecha, N., et al., *Interaction of the type Ialpha PIPkinase with phospholipase D: a role for the local generation of phosphatidylinositol 4, 5-bisphosphate in the regulation of PLD2 activity.* EMBO J, 2000. **19**(20): p. 5440-5449.
23. Denzin, L.K., et al., *Assembly and intracellular transport of HLA-DM and correction of the class II antigen-processing defect in T2 cells.* Immunity, 1994. **1**(7): p. 595-606.
24. Lampson, L.A. and R. Levy, *Two populations of Ia-like molecules on a human B cell line.* J.Immunol., 1980. **125**(1): p. 293-299.
25. Vennegoor, C. and P. Rumke, *Circulating melanoma-associated antigen detected by monoclonal antibody NKI/C-3.* Cancer Immunol Immunother, 1986. **23**(2): p. 93-100.
26. Neefjes, J.J., et al., *The biosynthetic pathway of MHC class II but not class I molecules intersects the endocytic route.* Cell, 1990. **61**(1): p. 171-183.
27. Peters, P.J., et al., *Segregation of MHC class II molecules from MHC class I molecules in the Golgi complex for transport to lysosomal compartments.* Nature, 1991. **349**(6311): p. 669-676.
28. Rocha, N., et al., *Cholesterol sensor ORP1L contacts the ER protein VAP to control Rab7-RILP-p150 Glued and late endosome positioning.* J Cell Biol, 2009. **185**(7): p. 1209-1225.
29. Boutros, M., L.P. Bras, and W. Huber, *Analysis of cell-based RNAi screens.* Genome Biol., 2006. **7**(7): p. R66.
30. Ten Brinke, A., et al., *The clinical grade maturation cocktail monophosphoryl lipid A plus IFNgamma generates monocyte-derived dendritic cells with the capacity to migrate and induce Th1 polarization.* Vaccine, 2007. **25**(41): p. 7145-7152.
31. Souwer, Y., et al., *B cell receptor-mediated internalization of salmonella: a novel pathway for autonomous B cell activation and antibody production.* J Immunol, 2009. **182**(12): p. 7473-7481.
32. Jordens, I., et al., *The Rab7 effector protein RILP controls lysosomal transport by inducing the recruitment of dynein-dynactin motors.* Curr Biol, 2001. **11**(21): p. 1680-1685.
33. Carpenter, A., et al., *CellProfiler: image analysis software for identifying and quantifying cell phenotypes.* Genome Biology, 2006. **7**(10): p. R100.
34. Wang, X. and M. McManus, *Lentivirus production.* J Vis Exp, 2009(32).